Research Article J. Electrochem. Sci. Technol., 2020, 11(4), 406-410

MnO_2 Nanowires Electrodeposited in a Porous Network of Agarose Gel as a Pseudocapacitor Electrode

Sohyun Jin[1†], Ilhwan Ryu[1†], Geo Lim[2], and Sanggyu Yim[1*]
[1]Department of Chemistry, Kookmin University, Seoul 02707, Korea
[2]Department of Biology, Boston University, Boston, MA 02215, U.S.A.

ABSTRACT

Despite a simple preparation of manganese oxide (MnO_2) nanowires by electrodeposition, the improvement in specific capacitance (C_{sp}) and voltammetric response of the MnO_2 nanowire-based electrodes has been quite limited. This is attributed to the poor electrical conductivity of MnO_2 and its dense bulk morphology due to the aggregation of the nanowires. This study investigated the capacitive performance of MnO_2 nanowires electrodeposited on agarose thin films. The good ionic conductivity and porous network of the agarose film provided favorable growth conditions for the MnO_2 nanowires with suppressed aggregation. A maximum C_{sp} value of 686 F/g measured at a scan rate of 10 mV/s was obtained, which was significantly larger than that of 314 F/g for the agarose-free MnO_2 electrode at the same scan rate. The rate capability was also improved. The C_{sp} measured at a high scan rate of 100 mV/s retained 74.0% of the value measured at 10 mV/s, superior to the retention of 71.1% for the agarose-free MnO_2 electrode.

Keywords : Pseudocapacitor, Manganese Oxide, Agarose Gel, Porous Network

Received : 3 February 2020, Accepted : 30 July 2020

1. Introduction

Supercapacitors are attracting increasing attention as a promising alternative to the current secondary batteries due to their high power density, long cycle life and rapid charge-discharge rate [1-3]. There are two types of supercapacitors, namely an electrical double layer capacitor (EDLC) and a pseudocapacitor, depending on the electrode material and charge storage mechanism. While carbon-based materials, representatively activated carbon, are used as the electrode material for EDLCs, transition metal oxides and conductive polymers are mainly used for pseudocapacitors [3-5]. In EDLCs, the charges are only stored electrostatically by the adsorption of ions on the electrode surface. In contrast, pseudocapacitors use the Faradaic redox reactions of the electrode materials as well and hence, have a significantly larger theoretical specific capacitance, C_{sp}, compared to the EDLCs.

Among the various electrode materials for pseudocapacitors, manganese oxide (MnO_2) is one of the most promising candidates due to its high theoretical C_{sp} of 1370 F/g, low price and environmentally friendly nature [1,6,7]. However, the capacitive properties, such as the specific capacitance and voltammetric response, of the MnO_2 electrode decrease rapidly as the electrode thickness increases due to its poor electrical conductivity and slow charge transport characteristics [6-9]. In this context, various MnO_2 nanostructure-based electrodes have been proposed to increase the contact between the electrode and electrolyte [8-12]. Representatively, MnO_2 nanowires have been most extensively studied because they can be easily fabricated on various substrates by a simple electrodeposition technique. However, due to the intrinsically dense morphology of the bulk MnO_2, the benefit of the nanostructure was only effective at the electrode surface, and hence, the improvement of the capacitive performance was quite limited.

In this study, we introduce a new nanostructure-

†These authors contributed equally to this work.
*E-mail address: sgyim@kookmin.ac.kr
DOI: https://doi.org/10.33961/jecst.2020.00759

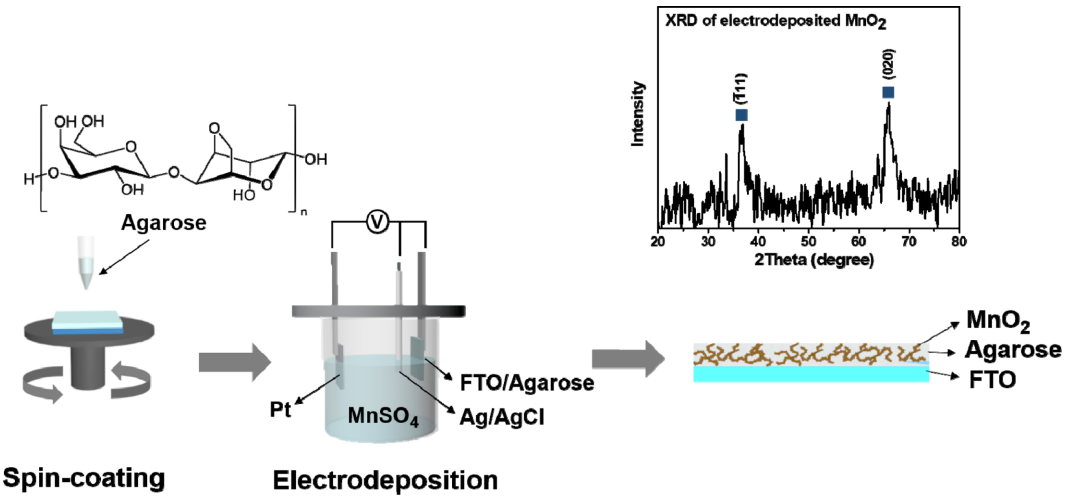

Fig. 1. Molecular structure of agarose and schematic illustration representing the fabrication of MnO_2–agarose electrodes. The powder X-ray diffraction pattern of the electrodeposited MnO_2 thin film is also shown.

based composite electrode fabricated by electrodepositing MnO_2 nanowires in a porous network consisting of a pre-coated agarose gel layer. Agarose is a linear polysaccharide consisting of alternating 1,3-linked-D-galactose and 1,4-linked-3,6-anhydro-L-galactose units [13,14]. The solidified agarose forms a water-containing gel with a 3D porous nanostructure generated by the cross-linking of molecules via hydrogen bonding [15,16]. Agarose gel is a soft, low-cost and biocompatible medium with a good ionic conductivity [17,18].

We found that the electrodeposition of MnO_2 in the 3D porous network of the agarose gel could effectively prevent the dense aggregation of the MnO_2 nanowires. As a result, the specific capacitance of the electrode and its retention at high scan rates significantly improved compared to the agarose-free MnO_2 nanowire-based electrode. Because the agarose gel can also be used as a gel electrolyte for supercapacitors [19], this MnO_2-agarose composite is a promising candidate for a one-body electrode-electrolyte component for flexible, solid-state supercapacitors.

2. Materials and Methods

A fluorine-doped tin oxide (FTO) substrate (sheet resistance of 7 Ω/sq.) was thoroughly cleaned using deionized water, acetone and isopropyl alcohol in an ultrasonic bath and blown dry with N_2 gas, followed by additional UV-ozone cleaning for 10 min. The 0.5 g agarose powder (Bioneer®) was dissolved completely in 50 mL boiling water with vigorous stirring, and then, the solution was spin-casted onto the cleaned FTO substrate at 3000 rpm for 20 s. After cooling down to room temperature, the transparent agarose gel layer was formed on the FTO substrate. The electrodeposition of the MnO_2 nanowires on the agarose gel-coated FTO substrate was done with a three electrode system shown in Fig. 1. An FTO substrate as a working electrode, a platinum plate as a counter electrode and Ag/AgCl in aqueous KCl solution as a reference electrode were used. In an aqueous electrolyte solution containing 5.0 mM manganese sulfate monohydrate ($MnSO_4 \cdot H_2O$) and 0.1 M sodium sulfate (Na_2SO_4), a cyclic potential between 0.4 and 1.3 V was applied repeatedly at a scan rate of 30 mV/s. After the electrodeposition, the electrode was washed with distilled water several times and dried at 60°C for 2 h. For comparison, MnO_2 nanowires were also electrodeposited on agarose-free ITO substrates using the same procedure, and their capacitive properties were investigated. The deposit weights of the MnO_2 nanowires were determined by a quartz crystal microbalance (QCM, Stanford Research Systems QCM200). The electronic absorption of the electrodes was investigated using a UV-vis spectrophotometer (S-3000, Scinco). The surface and cross-sectional morphology of the electrode films

were characterized by field emission scanning electron microscopy (FE-SEM, JSM-7410F, JEOL Ltd.) equipped with energy dispersive spectrometry (EDS). The capacitive properties of the fabricated electrodes were evaluated in 1.0 M aqueous Na_2SO_4 solution at room temperature using a cyclic voltammeter (ZIVE SP2, WonATech). The electrochemical impedance spectroscopy (EIS) measurements were also conducted at an open-circuit voltage of 200.5 mV amplitude to evaluate resistive elements of the electrodes.

3. Results and Discussion

Figs. 2(a) and 2(b) show the surface FE-SEM images of 30 cycle-electrodeposited MnO_2 electrodes on a bare and agarose-coated FTO substrate, respectively. The nanowires a few nanometers in width, characteristic of the electrodeposited MnO_2 [8,9,11], were clearly observed on the bare FTO substrate (Fig. 2a). In contrast, the electrodeposited MnO_2 onto the agarose layer had a blurry and less apparent nanowire shape (Fig. 2b). This is probably due to the growth of the MnO_2 in the porous network of the agarose gel. The 1 wt% agarose gel was reported to be a good ionic conductor with a pore size of several hundred nanometers [20], thus providing favorable conditions for the growth of the MnO_2 nanowires. The electrodeposited MnO_2 nanowires appeared to have bernessite-type crystallinity (JCPDS no. 80-1098), given that the diffraction peaks were observed at 2θ of 38° and 66°, as shown in the inset of Fig. 1 [8,21]. Elemental EDS mapping of the MnO_2–agarose layer in the cross-sectional SEM image also indicated that the MnO_2 nanowires were successfully and uniformly deposited over the entire film (Fig. 2c). This is somewhat different from the previously reported result that the electrodeposited MnO_2 using $Mn(NO_3)_2$ precursor solution on an agarose-coated stainless steel (SS) substrate formed three-layered structure (agarose gel/ MnO_2/SS) as the deposited MnO_2 layer pushed up the agarose gel layer [22]. The growth rate of MnO_2 nanowires seemed to be slightly slowed on the agarose gel. This is probably because the electrical conductivity of the agarose gel, 0.04 – 0.4 S/m depending on the concentration of electrolyte [23], is lower than that of the FTO, approximately 4.1 mΩ·cm (equaling to 2.4×10^5 S/m) [24]. After 30 cycles of electrodeposition on the bare and agarose-coated FTO substrates, the deposition weights estimated by a quartz crystal microbalance (QCM) were 85 and 53 mg/cm^2, respectively. The electronic absorption spectra and photographs also support these results (Fig. 2d).

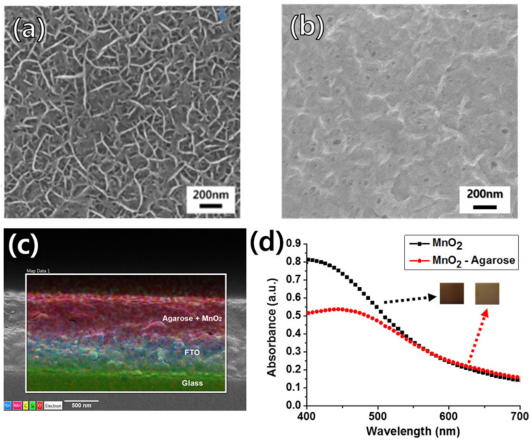

Fig. 2. Surface FE-SEM images of the (a) agarose-free MnO_2 and (b) MnO_2–agarose electrode taken after 30 cycles of electrodeposition. The cross-sectional FE-SEM image and elemental EDS mapping of the MnO_2–agarose electrode (c) and electronic absorption spectra of both electrodes (d) are also presented. The photographs of the fabricated electrodes are shown in (d) as an inset.

Cyclic voltammetry of the 30 cycle-electrodeposited MnO_2 electrodes was carried out in a 1.0 M aqueous Na_2SO_4 solution at a potential range between 0.0 V and 0.8 V. Figs. 3(a) and 3(b) show the cyclic voltammograms (CVs) measured at various scan rates for the agarose-free MnO_2 and MnO_2–agarose electrode, respectively. The areal capacitance, C_{areal}, of the electrodes was calculated according to the following equation;

$$C_{areal} = \frac{\int JdV}{\Delta V(dV/dt)} \quad (1)$$

where J (mA/cm^2) is the areal current; ΔV (V) is the potential window, and dV/dt (mV/s) is the scan rate. At the slowest scan rate of 10 mV/s, the largest C_{areal} values were obtained for both types of the electrodes. Interestingly, the C_{areal} of the MnO_2–agarose electrode (36.5 mF/cm^2) was approximately 1.4 times larger than that of the agarose-free MnO_2 electrode (26.7 F/cm^2) despite that the deposited MnO_2 weight is 1.6 times smaller. Since the areal capaci-

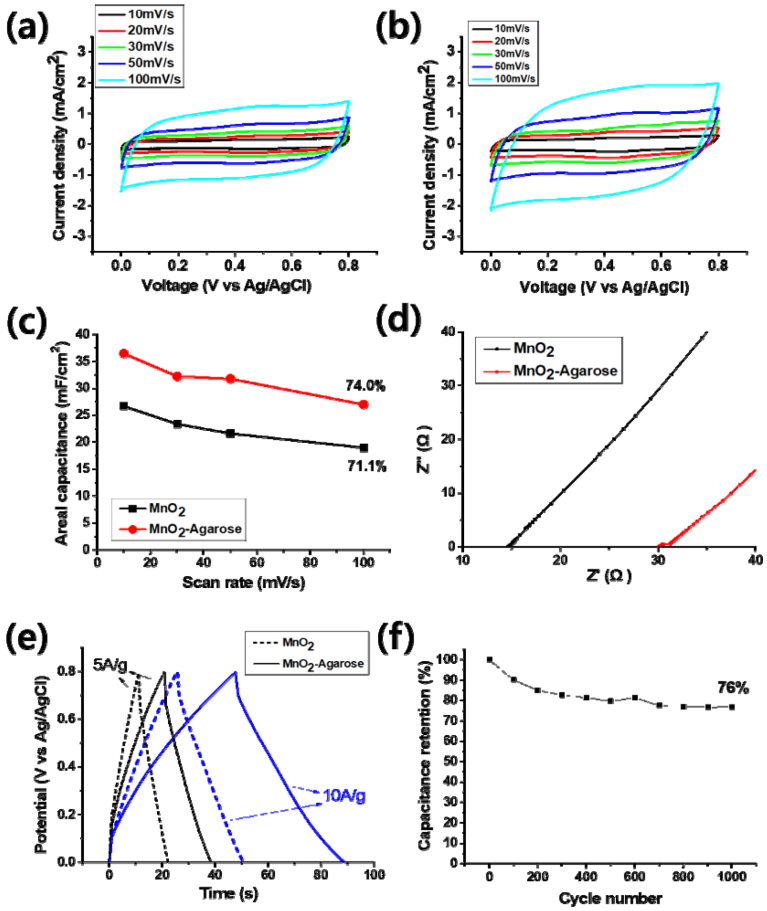

Fig. 3. Cyclic voltammograms of the 30 cycle-electrodeposited (a) agarose-free MnO_2 and (b) MnO_2–agarose electrodes measured at various scan rates. The calculated C_{areal} values of the electrodes are plotted as a function of the scan rate in (c). (d) Nyquist plots for the agarose-free MnO_2 and MnO_2–agarose electrodes. (e) GCD curves of the electrodes measured at a current densities of 5 and 10 A/g. (f) Capacitance retention of the MnO_2–agarose electrode as a function of the number of GCD cycles.

tance rarely decreases as the mass of the deposited electrode material increases, this larger C_{areal} value even with smaller MnO_2 deposition apparently indicates the superiority of the MnO_2–agarose electrode to the agarose-free MnO_2 electrode. Owing to the increased C_{areal} with smaller deposit mass, the specific capacitance, C_{sp}, of the MnO_2–agarose electrode (686 F/g) was significantly larger than that of the agarose-free MnO_2 electrode (314 F/g). The enhancement of these capacitive properties is probably attributed to the increased contact with the electrolyte. Another advantage of the suppressed aggregation during the electrodeposition is an improvement in the voltammetric response at high scan rates. The specific capacitance of both the electrodes gradually decreased as the scan rate increased shown in Fig. 3(c). For the agarose-free MnO_2 electrode, the C_{sp} at a scan rate of 100 mV/s was 223 F/g; thus, the retention from the value at a scan rate of 10 mV/s was 71.1%. For the MnO_2–agarose electrode, the C_{sp} measured at 100 mV/s was 508 F/g with a retention of 74.0%. The resistive elements of the electrodes were evaluated by EIS measurements. The Nyquist plots shown in Fig. 3(d) indicated that the series resistance of the MnO_2–agarose electrode is approximately twice larger than that of the agarose-free MnO_2 electrode. However, the diffusive resistance, R_d, which is inversely proportional to the slope of the

line, of the two electrodes was similar. The capacitive performance of the MnO_2 electrodes was also tested by galvanostatic charge-discharge (GCD) measurements (Fig. 3e). While the C_{sp} value of the agarose-free MnO_2 electrode was 131 F/g measured at a current density of 5 A/g, that of the MnO_2–agarose electrode was 201 F/g at the same measurement condition. At the higher current density of 10 A/g, the C_{sp} values were 114 and 178 F/g, respectively. The significantly longer discharge time of the MnO_2–agarose electrode indicates the better charge storage capability of the MnO_2 nanowires grown in the porous agarose network. The C_{sp} retention of the MnO_2–agarose electrode was approximately 76% of the initial value after 1000 GCD cycles (Fig. 3f).

4. Conclusions

In summary, an aggregation-suppressed MnO_2 nanostructure electrode was successfully fabricated by electrodepositing MnO_2 nanowires in a pre-coated agarose thin film. The 3D porous network of the agarose layer could provide favorable growth conditions for the MnO_2 nanowires in terms of the space and ionic conductivity while preventing aggregation between them. The highest C_{sp} value of the MnO_2–agarose electrode was 686 F/g measured at a scan rate of 10 mV/s, which was significantly larger than 314 F/g of the agarose-free MnO_2 electrode measured at the same condition. The C_{sp} values obtained from the GCD measurements also supported the large improvement of the charge storage capability of the MnO_2–agarose electrode. The voltammetric response of the MnO_2–agarose electrode was also improved. The C_{sp} of the MnO_2–agarose electrode retained 74.0% at a high scan rate of 100 mV/s, which is larger than the retention of 71.1% for the agarose-free MnO_2 electrode. All these results, a considerably enhanced specific capacitance with a larger retention, clearly demonstrate the effectiveness of the suppressed aggregation of MnO_2 nanowires grown in an agarose gel and the benefits of the resulting MnO_2–agarose electrode.

Acknowledgement

This work was supported by National Research Foundation of Korea (NRF) Grants (No. 2016R1A5A1012966) funded by the Korean Government.

References

[1] Poonam, K. Sharma, A. Arora, S. K. Tripathi, *J. Energy Storage*, **2019**, *21*, 801–825.
[2] A. González, E. Goikolea, J.A. Barrena, R. Mysyk, *Renew. Sustain. Energy Rev.*, **2016**, *58*, 1189–1206
[3] G. Wang, L. Zhang, J. Zhang, *Chem. Soc. Rev.*, **2012**, *41(2)*, 797-828.
[4] X. Peng, L. Peng, C. Wu, Y. Xie, *Chem. Soc. Rev.*, **2014**, *43(10)*, 3303-3323.
[5] E. E. Miller, Y. Hua, H. Tezel, *J. Energy Storage*, **2018**, *20*, 30-40.
[6] M. Toupin, T. Brousse, D. Bélanger, *Chem. Mater.*, **2004**, *16*, 3184-3190.
[7] K. Zhang, X. Han, Z. Hu, X. Zhang, Z. Tao, J. Chen, *Chem. Soc. Rev.*, **2015**, *44(3)*, 699-728.
[8] I. Ryu, G. Kim, H. Yoon, S. Ahn, S. Yim, *RSC Adv.*, **2016**, *6(104)*, 102814-102820.
[9] G. Kim, I. Ryu, S. Yim, *Sci. Rep.*, **2017**, *7*, 8260.
[10] W. Xiao, H. Xia, J. Y.H. Fuh, L. Lu, *J. Power Sources*, **2009**, *193(2)*, 935-938.
[11] S. O. Ranaei Siadat, *J. Electrochem. Sci. Technol.*, **2015**, *6(3)*, 81-87.
[12] J. Wei, N. Nagarajan, I. Zhitomirsky, *J. Mater. Process Technol.*, **2007**, *186(1-3)*, 356-361.
[13] S-K. Kamaraj, S. M. Romano, V. C. Moreno, H. M. Poggi-Varaldo, O. Solorza-Feria, *Electrochim. Acta*, **2015**, *176*, 555-566.
[14] D. F. Vieira, C. O. Avellaneda, A. Pawlicka, *Electrochim. Acta*, **2007**, *53(4)*, 1404-1408.
[15] J. G. Clar, C. A. Silvera Batista, S. Youn, J-C. J. Bonzongo, K. J. Ziegler, *J. Am. Chem. Soc.*, **2013**, *135(47)*, 17758-17767.
[16] X. Wang, C. E. Egan, M. Zhou, K. Prince, D. R. G. Mitchell, R. A. Caruso, *Chem. Commun.*, **2007**, *29*, 3060-3062.
[17] C. Özdemir, A. Güner, *Eur. Polym. J.*, **2007**, *43(7)*, 3068-3093.
[18] C. Duffus, P. J. Camp, A. J. Alexander, *J. Am. Chem. Soc.*, **2009**, *131(33)*, 11676-11677.
[19] W. Moon, G. Kim, M. Lee, H. Song, J. Yi, *ACS Appl. Mater. Interfaces*, **2015**, *7(6)*, 3503-3511.
[20] N. Pernodet, M. Maaloum, B. Tinland, *Electrophoresis*, **1997**, *18(1)*, 55-58.
[21] H. Le, S. Jin, S. Yim, *J. Phys. Chem. Solids*, **2020**, *138*, 109264.
[22] S. Park, I. Nam, G-P. Kim, J. W. Han, J. Yi, *ACS Appl. Mater. Interfaces*, **2013**, *5(20)*, 9908-9912.
[23] M. A. Kandadai, J. L. Raymond, G. J. Shaw, *Mater. Sci. Eng. C Mater. Biol. Appl.*, **2012**, *32(8)*, 2664-2667.
[24] L. T. C. Tuyen, S-R. Jian, N. T. Tien, P. H. Le, *Mater.*, **2019**, *12(10)*, 1665.